BioMACROMOLECULES

pubs.acs.org/Biomac Article

Synthesis of Silver Nanoparticles Using Curcumin-Cyclodextrins Loaded into Bacterial Cellulose-Based Hydrogels for Wound Dressing Applications

Abhishek Gupta,* Sophie M. Briffa, Sam Swingler, Hazel Gibson, Vinodh Kannappan, Grazyna Adamus, Marek Kowalczuk,* Claire Martin, and Iza Radecka*

Cite This: *Biomacromolecules* 2020, 21, 1802−1811

Read Online

ACCESS | Metrics & More | Article Recommendations

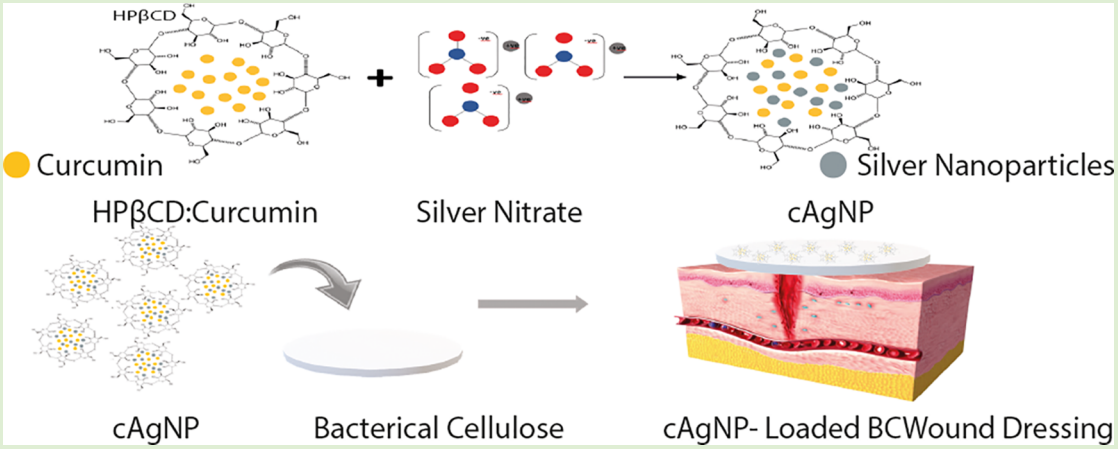

ABSTRACT: Chronic wounds are often recalcitrant to treatment because of high microbial bioburden and the problem of microbial resistance. Silver is a broad-spectrum natural antimicrobial agent with wide applications extending to proprietary wound dressings. Recently, silver nanoparticles have attracted attention in wound management. In the current study, the green synthesis of nanoparticles was accomplished using a natural reducing agent, curcumin, which is a natural polyphenolic compound that is well-known as a wound-healing agent. The hydrophobicity of curcumin was overcome by its microencapsulation in cyclodextrins. This study demonstrates the production, characterization of silver nanoparticles using aqueous curcumin:hydroxypropyl-β-cyclodextrin complex and loading them into bacterial cellulose hydrogel with moist wound-healing properties. These silver nanoparticle-loaded bacterial cellulose hydrogels were characterized for wound-management applications. In addition to high cytocompatibility, these novel dressings exhibited antimicrobial activity against three common wound-infecting pathogenic microbes *Staphylococcus aureus*, *Pseudomonas aeruginosa*, and *Candida auris*.

INTRODUCTION

Microbial colonization, where it is not wanted, can led to severe infections which can result in disability, disease, and even death. Wound infections are one of the major factors resulting in impaired healing.[1−3] Wounds colonized by opportunistic microbes may fail to follow the natural reparative and regenerative stages involved in the healing process.[4] In addition, uncontrolled infections can prevent the restoration of the anatomical and physiological integrity resulting in chronic nonhealing wounds.[5,6] To prevent infections, modern medicine is dependent on antimicrobial agents such as antibiotics which can either destroy pathogens or inhibit their growth. Unfortunately, the misuse of antibiotics has resulted in the emergence of a number of multiresistant microbes. Therefore, antibiotic therapy often proves to be ineffective in eradicating infections in chronic nonhealing wounds.[3] Owing to the site specific delivery, increased target site concentration, reduced adverse effects, use of agents not suitable for oral and systemic therapy and low incidence of resistance,[7,8] antimicrobial-loaded wound dressings have attracted wide interest as a concurrent wound-management regime.

Special Issue: Anselme Payen Award Special Issue

Received: December 13, 2019
Revised: January 21, 2020
Published: January 22, 2020

https://dx.doi.org/10.1021/acs.biomac.9b01724
Biomacromolecules 2020, 21, 1802−1811

Hydrogels are one of the promising candidates as wound dressings because of their unprecedented properties including their ability to maintain a moist microclimate at the wound site which is proven to facilitate healing.[9−11] A number of natural and synthetic polymeric materials are in use to produce hydrogel dressings.[12,13] Bacterial cellulose (BC) is an example of a natural biosynthetic cellulose hydrogel which has been widely considered as a wound dressing because of its unique properties.[14−18] BC can be produced by several bacteria, but *Gluconacetobacter xylinus* (*G. xylinus*) is considered as one of the best for BC production.[19] Our group has previously reported the findings on the physicochemical characterization and suitability of BC hydrogels as wound dressings.[20] Although BC does not have inherent antimicrobial activity, however, its cross-linked fiber network structure encouraged several research attempts of loading antimicrobials, anti-inflammatory, antioxidants, and other healing agents for wound-dressing applications.[17,21,22] In continuation, in the presented study, an investigation has been made to produce biosynthetic hydrogels with healing properties for chronic wound management. Our novel approach is consistent with the concept of the forensic engineering of advanced polymeric materials (FEAPM) which can help to understand the relationships between the structure of the biomaterial used, its properties, and behavior for practical applications.[23]

Currently the treatment of microbial infections is severely affected by the emergence of new multiresistant microbes, including bacteria and fungi. Gram-positive *Staphylococcus aureus* has a great ability to develop multiple drug resistances. Similarly, Gram-negative *Pseudomonas aeruginosa*, a common opportunistic pathogen shows resistance to most penicillins, cephalosporins, and carbapenems. Pathogenic fungi such as *Candida auris* pose a significant health risk to patients suffering from infected wounds and in particular to immunocompromised individuals which can result in candidiasis/candidemia and invasive aspergillosis. Recently, a new multidrug-resistant strain of *C. auris* was discovered[24] and has quickly become a prolific nosocomial pathogen in the U.K.,[25,26] with diagnoses on all continents with 33 countries reporting incidents of antifungal resistance. *C. auris* is resistant to most first- and second-generation antifungals with 90% of isolates being resistant to fluconazole, 40% resistant to amphotericin and 2% to echinocandins such as caspofungin.[27−29] The concern regarding these pathogens centers around the increasing resistance they are showing toward a very limited pool of effective antimicrobials,[30−32] and hence, the focus is on targeted delivery by antimicrobial wound dressings.

Silver is a well-known antimicrobial effective against fungi, yeast, and bacteria including several antibiotic-resistant strains.[33−35] The emergence of nanotechnology enabling the production of silver nanoparticles has served a new therapeutic modality. Because of their characteristic broad-spectrum antimicrobial properties, silver nanoparticles (AgNP) have received increased focus in biomedical applications including for wound management.[36−38] Among the several different approaches to synthesize AgNP, the use of natural substances like plant extracts has received wide research consideration because of the safe and eco-friendly procedure.[37,39−41]

Curcumin (CUR), a natural polyphenol extracted from turmeric, is a well-known wound-healing agent with proven antimicrobial, antioxidant, and anti-inflammatory effects.[22,42] In addition to its healing properties, CUR has been used as a reducing and capping agent to produce AgNP.[43] The main challenge that limits the wider biomedical application of CUR is its hydrophobic nature. Several chemical mediators like dimethyl sulfoxide, dichloromethane, and sodium carbonate are employed in AgNP synthesis from CUR.[44−48] These chemical mediators can have serious cytotoxic effects.[48] Selection of solvent medium, reducing agent, and nontoxic stabilizer are the main considerations in green nanoparticle production.[49,50] The current study reports the production of AgNP following a green chemistry approach using an aqueous solution of curcumin:hydroxypropyl-β-cyclodextrin (CUR:HPβCD). These AgNP produced using CUR:HPβCD (cAgNP) were characterized and loaded in the biosynthetic BC hydrogels to produce hydrogel dressings. To the best of our knowledge, the protocol presented herein to produce cAgNP is novel, and this is the first time the production of cAgNP-loaded BC has been reported. This report presents the unique combination of silver nanoparticles with curcumin in the biosynthetic BC to obtain the hydrogels for wound-management applications. This study investigates the inherent antimicrobial, antioxidant, and cytocompatibility properties of these novel hydrogel dressings.

MATERIALS AND METHODS

Materials. *Gluconoacetobacter xylinus* (ATCC 23770), *Pseudomonas aeruginosa* (NCIMB 8295), and *Staphylococcus aureus* (NCIMB 6571) were obtained from the University of Wolverhampton culture collection. *Candida auris* (NCF 8971) was obtained from the Public Health England Culture Collection, Porton Down, U.K. A stock culture of *P. aeruginosa* and *S. aureus* were resuscitated at 37 °C on tryptone soy agar (TSA) (Sigma-Aldrich, U.K.), *G. xylinus* at 30 °C on mannitol agar, and *C. auris* at 37 °C on Sabouraud Dextrose Agar (SDA). HS media was prepared following the standard protocol.[51] Material for mannitol agar, SDA, and HS media were purchased from Lab M (U.K.). Tryptone soya broth (TSB), disodium phosphate, and citric acid were purchased from Sigma-Aldrich (U.K.). Overnight broth cultures were prepared in appropriate medium using the stock plates.

U251MG (U251), MSTO and Panc 1 cell lines were purchased from ATCC (U.K.). Defibrinated horse whole blood was purchased from TCS Biosciences Ltd.

Silver nitrate was purchased from Fischer Scientific (U.K.). Hydroxypropyl-β-cyclodextrin (parenteral grade) was kindly provided by Roquette (France). Curcumin and dimethyl sulfoxide (DMSO) (spectrophotometric grade) were purchased from Alfa Aesar (U.K.). Ringer tablets were purchased from Lab M (U.K.). Thiazolyl Blue Tetrazolium Bromide (MTT), sodium bicarbonate, and 2,2-diphenyl-1-picrylhydrazyl (DPPH) were purchased from Sigma-Aldrich (U.K.). Sodium chloride 0.9% (w/v) (normal saline, intravenous infusion) was purchased from Baxter, U.K. Sodium hydroxide was purchased from Acros Organics (U.K.). NaCl (5.8 g/L) and glycine (7.6 g/L) for preparing Sorensen's glycine buffer were purchased from Sigma-Aldrich, U.K. Trypsin was purchased from Lonza (Belgium). Dulbecco's Modified Eagle's Medium (DMEM), fetal bovine serum (FBS), L-glutamine, and antibiotic antimycotic were purchased from Gibco (U.K.).

Preparation of CUR:HPβCD Inclusion Complex. Inclusion complex was synthesized by the solvent evaporation method following the protocol previously reported.[22] Briefly, CUR solution (0.79 g in 37.5 mL acetone) was added dropwise to the aqueous HPβCD solution (3.0 g in 12.5 mL deionized water) under constant stirring at room temperature for slow and complete evaporation of acetone. The sample was centrifuged, and the aqueous supernatant containing CUR:HPβCD inclusion complex was frozen after filtration and lyophilized.

Preparation and Characterization of cAgNP. *Preparation of cAgNP Using CUR:HPβCD.* A novel green chemistry approach was developed for cAgNP synthesis by reducing silver nitrate ($AgNO_3$)

https://dx.doi.org/10.1021/acs.biomac.9b01724
Biomacromolecules 2020, 21, 1802−1811

with an aqueous solution of CUR:HPβCD. CUR:HPβCD (0.19 g) solution was prepared by dissolving in deionized water (18 mL). CUR:HPβCD aqueous solution was added dropwise with constant stirring to 1 mM $AgNO_3$ aqueous solution (42 mL) under the boiling condition in conical flasks. The mixed solutions were boiled for 3 h for reduction of Ag ions followed by cooling at room temperature for 30 min. The flask was covered with aluminum foil to maintain dark conditions throughout the reduction process to avoid any photochemical reactions.

Characterization of cAgNP. *Dynamic Light Scattering (DLS) and Zeta Potential.* DLS measurements were performed on a Malvern Zetasizer (nano ZS) at the University of Birmingham. Five consecutive measurements were carried out at 25 °C with samples equilibrated for 2 min before the measurements were started. The results were averaged to calculate the mean size. The same instrument was used to obtain the Zeta Potential values. The same samples were used for size measurements and equilibrated for 2 min before measurements were started. The results were obtained at 25 °C. Five consecutive measurements were taken and averaged to calculate the zeta potential.

Transmission Electron Microscopy (TEM). The shape, size, and distribution of cAgNP produced using CUR:HPβCD were investigated by TEM. Briefly, a drop of aqueous colloidal cAgNP was casted on a carbon-coated 300 mesh copper grid (agar scientific), left for 30 min, rinsed off, and allowed to dry at room temperature in a covered container. TEM imaging was performed using JEOL 1400 electron microscope, operated at 80 keV. Images were captured at different range of magnifications. A 100 cAgNP were randomly selected and measured using ImageJ to obtain the size distribution.

Preparation of cAgNP-Loaded BC Hydrogels. Production of Bacterial Cellulose Hydrogels. Bacterial cellulose (BC) hydrogels were prepared by the protocol reported previously.[22] Briefly, *G. xylinus* was selected for BC production, and hydrogels were biosynthesized in sterilized Hestrin and Schramm (HS) culture medium under static condition. BC pellicles were purified prior to experimental use.

Loading cAgNP in BC Hydrogels. BC pellicles afterpurification were padded dry on sterilized filter paper and aseptically loaded with cAgNP by immersing in aqueous colloidal cAgNP overnight under agitated conditions at 4 °C.

Characterization Studies. *Morphological Study by Scanning Electron Microscopy (SEM).* Morphology of BC (neat) has been previously reported.[22,S2] BC before purification, purified BC (neat) and cAgNP-loaded BC hydrogels were cut in to discs (8 mm) using a biopsy punch and lyophilized. These discs were then coated with ultrafine gold coating using SC500 fine coater (Emscope, Kent, U.K.) and placed on a carbon stub. The morphology of the samples was studied using a Zeiss Evo 50 EP, SEM (Carl Zeiss AG, Oberkochen, Germany).

Energy-Dispersive X-ray (EDX) Analysis. Lyophilized cAgNP-loaded BC hydrogel samples were analyzed by EDX (Zeiss Evo 50 EP, SEM) coupled with X-Max^N 50 Silicon Drift Detector (Oxford Instruments), and the analysis was performed by Oxford Instruments INCA Energy Dispersive Spectroscopy Nanoanalysis software using the Point & ID function, to confirm the presence of silver.

Moisture Content (M_c). The wet mass (W_w) of BC (neat) and cAgNP-loaded BC (test) hydrogels was recorded before lyophilization, and the dry mass (W_d) was measured after 72 h of lyophilization. M_c (%) was calculated using a formula:

$$\%M_c = \frac{(W_w - W_d)}{W_w} \times 100$$

Cytocompatibility Study (In Vitro Cell Viability). Cytocompatibility of BC (neat) has been previously tested and reported using conditioned media[20] and BC discs[22] on different mammalian cell lines. To study the cytocompatibility of cAgNP-loaded BC, an *in vitro* cell viability test was performed using Panc 1 (human pancreatic ductal adenocarcinoma), U251 (human glioblastoma), and MSTO (human mesothelioma) following the protocol previously reported.[22]

All cell lines were cultured in Dulbecco's Modified Eagle's Medium (DMEM), supplemented with fetal bovine serum (FBS), antibiotic antimycotic, and L-glutamine at 37 °C in humidity incubator with 5% CO_2. BC pellicles after pad drying were either rehydrated with PBS (control) or cAgNP (test) overnight under agitated conditions (150 rpm) at 4 °C. These samples (control and test) were then aseptically cut in discs (8 mm) using a biopsy punch for experimental purposes, and the temperature was adjusted to 37 °C before use.

Briefly, 25 000 cells were seeded per well (24-well plate) for 24 h at 37 °C in 5% CO_2 incubator. The cells were exposed to either free cAgNP (equivalent amount) or cAgNP-loaded BC (8 mm discs) for 24 h to investigate the effect on cell viability. Cells without BC discs and PBS-loaded BC discs (8 mm) were used as controls, respectively. Cell viability was evaluated following the standard MTT assay previously reported.[22] Data recorded was analyzed statistically by two-way analysis of variance (ANOVA) with a Tukey's multicomparisons test using GraphPad Prism.

Hemocompatibility. The hemocompatibility of cAgNP-loaded BC hydrogels was tested following the protocol previously reported.[22] Briefly, defibrinated horse whole blood was washed twice using commercially available normal saline (pH 5.5), and blood cells were resuspended in normal saline. cAgNP-loaded BC discs (8 mm) were cut using a biopsy punch and incubated with 1.9 mL of horse blood cells suspended in normal saline in test Eppendorf tubes. The positive (+ve) control was blood cells suspended in distilled water and negative (−ve) control was blood cells in normal saline. All the test and control Eppendorf tubes were incubated at 4 °C for 2 h with periodic inversion (every 15 min). Postincubation, after the removal of BC discs from test Eppendorf tubes, all the tubes were centrifuged at 3000 rpm for 10 min at 4 °C. The supernatant was decanted and absorbance was recorded (540 nm) to calculate percentage hemolysis (% Hemolysis).

$$\%\text{Hemolysis} = \frac{(\text{Abs of sample}) - (\text{Abs of } -\text{ve control})}{(\text{Abs of } +\text{ve control}) - (\text{Abs of } -\text{ve control})} \times 100$$

Antimicrobial Study (Disc Diffusion Assay). The antimicrobial activity of cAgNP-loaded BC was investigated against *P. aeruginosa* (Gram−ve), *S. aureus* (Gram + ve) bacteria, and *C. auris* using the disc diffusion assay. PBS-loaded BC and HPβCD-loaded BC were used as controls. Discs (8 mm) of PBS-loaded BC, HPβCD-loaded BC, and cAgNP-loaded BC were placed aseptically on TSA plates spread with an overnight culture of *P. aeruginosa* or *S. aureus*, and SDA plates were spread with an overnight culture of *C. auris*. Plates were incubated at 37 °C for 24 h, and zones of inhibition (ZOI) were measured. Data is presented as mean ± standard deviation (SD) and analyzed statistically by two-way ANOVA with a Tukey's multi comparisons test using GraphPad Prism.

Antioxidant Study by DPPH Assay. The antioxidant potential of cAgNP produced using CUR:HPβCD was evaluated using 2,2-diphenyl-1-picrylhydrazyl (DPPH) radical scavenging assay. The assay mixture with 1 mL of DPPH (80 μg/mL) methanolic solution and 1 mL of test colloidal cAgNP (including the blank) after mixing were incubated for 30 min in the dark at room temperature. Absorbance was recorded (517 nm), and the free radical scavenging potential was calculated as percent antioxidant effect (% E) as

$$\%E = \frac{\text{Abs}_{\text{control}} - \text{Abs}_{\text{sample}}}{\text{Abs}_{\text{control}}} \times 100$$

Transparency Test. Monitoring the healing process without the need of removing dressing could help minimize trauma to the granulating tissue. With the aim to use the hydrogel as a wound-dressing application, the transparency level of cAgNP-loaded BC hydrogels was assessed by simulation. PBS-loaded BC and cAgNP-loaded-BC hydrogels were transferred on the laminated sheet of paper with text typed in different colors. The clarity of text underneath the hydrogel was examined to determine if the healing tissue at the wound site could be observed through these hydrogels.

https://dx.doi.org/10.1021/acs.biomac.9b01724
Biomacromolecules 2020, 21, 1802−1811

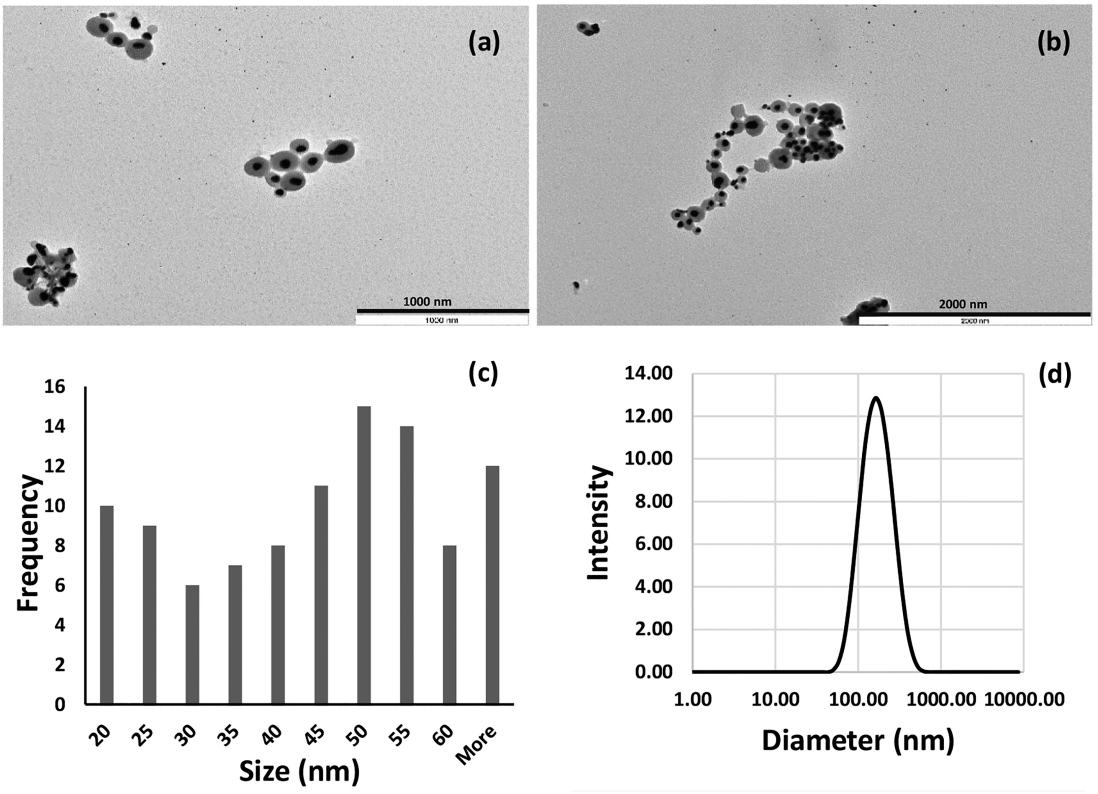

Figure 1. Characterization of cAgNP produced using CUR:HPβCD. (a,b) TEM photomicrographs. (c) Size distribution as measured by TEM analysis and calculated with 100 nanoparticles. (d) DLS data of cAgNP with size distribution.

RESULTS AND DISCUSSION

Preparation of cAgNP and cAgNP-Loaded BC Hydrogels. Most of the AgNP synthesis methods involve the use of organic solvents and toxic reducing agents with the potential threat to the environment and cytotoxic effect on mammalian cell lines. The method reported herein involved bioreduction of $AgNO_3$ with an aqueous solution of CUR:HPβCD resulting in nanoparticle formation. The color changed from colorless to pale yellow at the start of CUR:HPβCD addition which intensified with increased dosage and subsequently changed to yellow-brown with time, suggesting the production of nanoparticles. This could be due to the excitation of surface plasmon vibrations in AgNPs, which is in accordance with literature.[40,53]

G. xylinus produced BC hydrogel pellicles which were harvested and purified. BC pellicles became clear after purification. These results are in accordance with previous reports.[15,22,33,52,54] When the purified padded dry BC was rehydrated with the aqueous colloidal cAgNP, the pellicles reswelled and the color changed to yellow-brown. These cAgNP-loaded BC hydrogels were stored at 4 °C throughout the experimental procedure.

Characterization of cAgNP and cAgNP-Loaded BC Hydrogels. The formation of colloidal cAgNP produced was confirmed by testing its properties like size distribution and charge. After loading aqueous colloidal cAgNP in the padded dry BC, the physicochemical and *in vitro* hemocompatibility and cytocompatibility hydrogels were investigated.

Particle Size Distribution and Surface Charge by TEM, DLS, and Zeta Potential. The size and morphology of cAgNP produced using CUR:HPβCD were studied from the TEM images (Figure 1a–c). TEM imaging showed that the morphology of the nanoparticles was mainly spherical in shape with smooth edges. The majority of bioreduced cAgNP were in the diameter range of 20–55 nm (80%) and the average size of 42.71 ± 17.97 nm. (Figure 1a–c). It emerged from the results that nanoparticles were homogeneously surrounded by a thin layer of capping material. As the method employed in the current work involved only $AgNO_3$ and CUR:HPβCD, without the use of any organic solvents and additional capping agents, this suggests that CUR:HPβCD was acting both as a reducing and capping agent. These results are in agreement with literature reporting the use of curcumin as a reducing and capping agent.[40,43,46,48,53]

DLS measurements identified nanoparticles with the hydrodynamic diameter in the range of 182.10 ± 8.83 nm (Figure 1d) and the polydispersity index (PDI) value of 0.196 ± 0.009. These results indicate both nucleation to form new nanoparticles and aggregation could be happening consecutively. These findings are consistent with studies reported in the literature.[53,55] Low PDI indicates that the colloidal cAgNP was not very polydispersed.

The zeta potential value is directly proportional to the stability of nanoparticle dispersion.[55] Zeta potential studies revealed a negative charge on the synthesized nanoparticles with the magnitude of −20.1 ± 0.702 mV. These findings are in a close range to the previously reported values for AgNP bioreduced using curcumin.[43]

Scanning Electron Microscopy (SEM). BC has a fine fiber network structure with voids.[21,22,52] SEM images revealed *G. xylinus* trapped in the cellulose network before purification (Figure 2a) and that bacteria were successfully removed on

https://dx.doi.org/10.1021/acs.biomac.9b01724
Biomacromolecules 2020, 21, 1802–1811

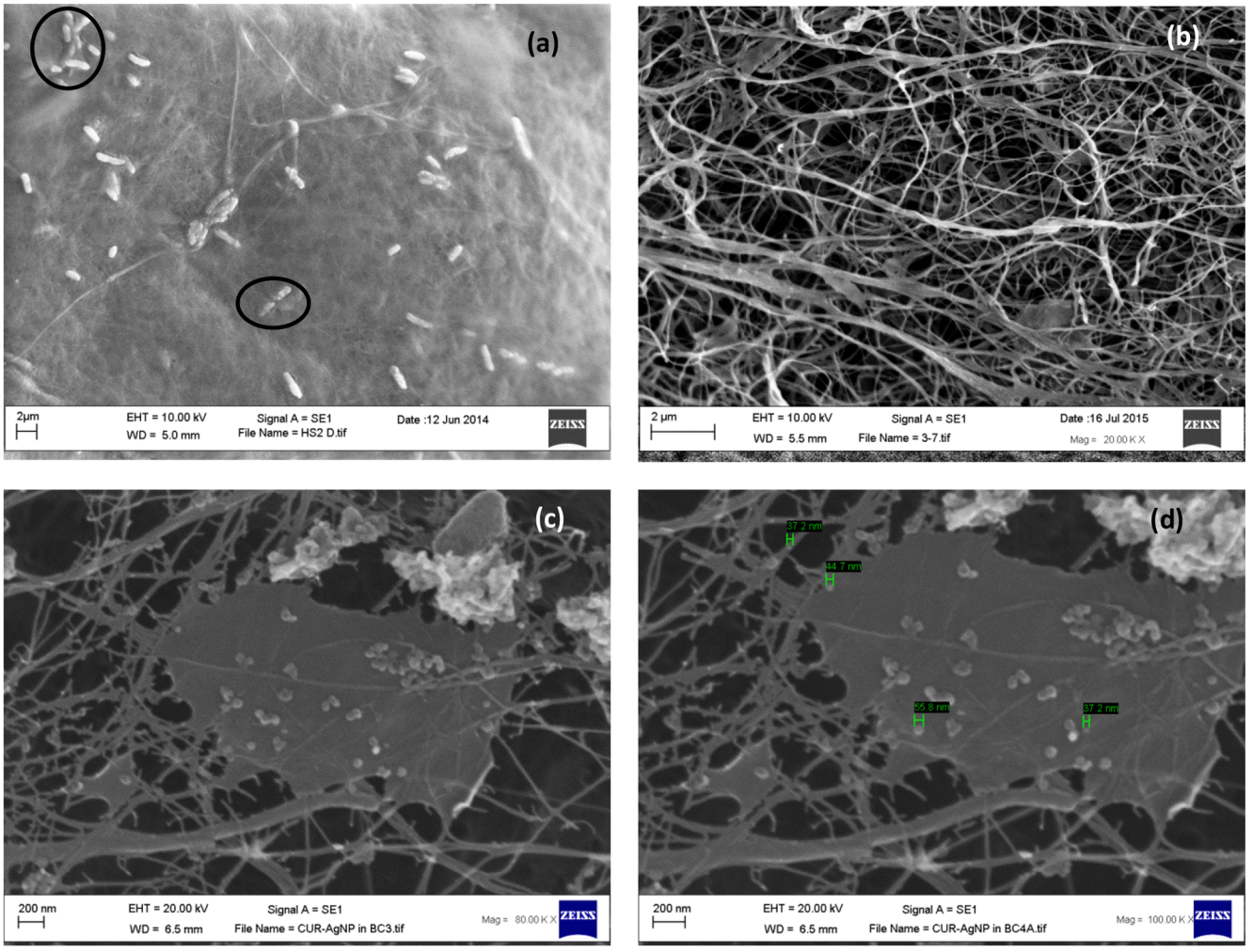

Figure 2. SEM photomicrographs of (a) unwashed BC, entangled *G. xylinus* highlighted. (b) BC after purification. (c,d) cAgNP loaded in BC fiber network.

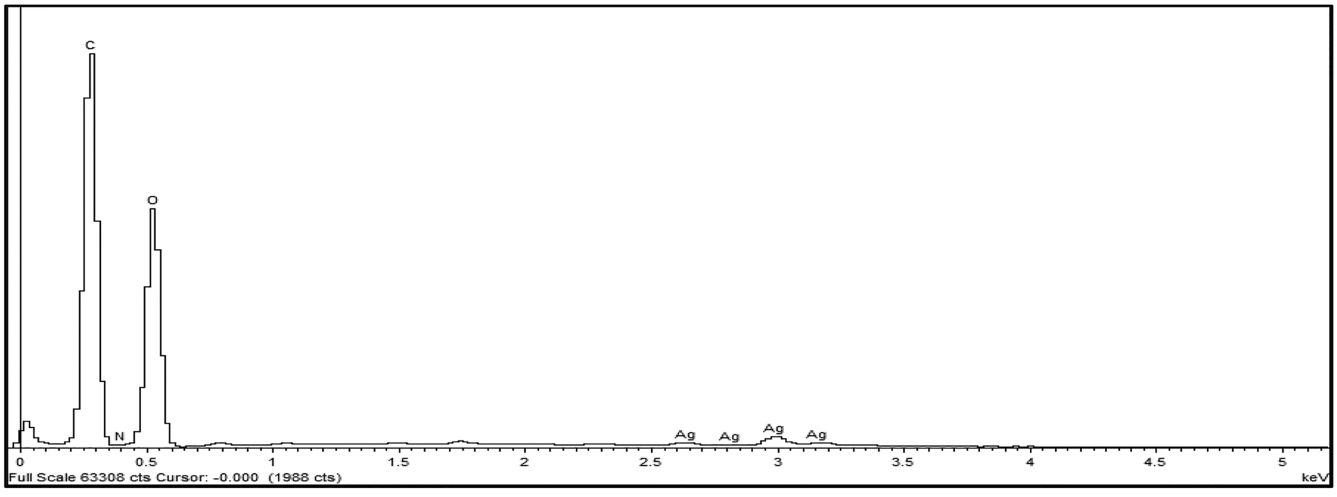

Figure 3. EDX spectrum of cAgNP-loaded BC.

purification (Figure 2b). The interspersed voids in the interwoven cellulose ribbons of BC allow impregnation of healing agents.[17,33,56] SEM of lyophilized cAgNP-loaded BC revealed that cAgNP penetrated through the voids during rehydration of padded dry BC pellicles and got physically trapped in the fiber network structure (Figure 2c). Also, it emerged that along with bioreduced cAgNP, there was free CUR:HPβCD trapped in the BC. In addition to the reducing

https://dx.doi.org/10.1021/acs.biomac.9b01724
Biomacromolecules 2020, 21, 1802−1811

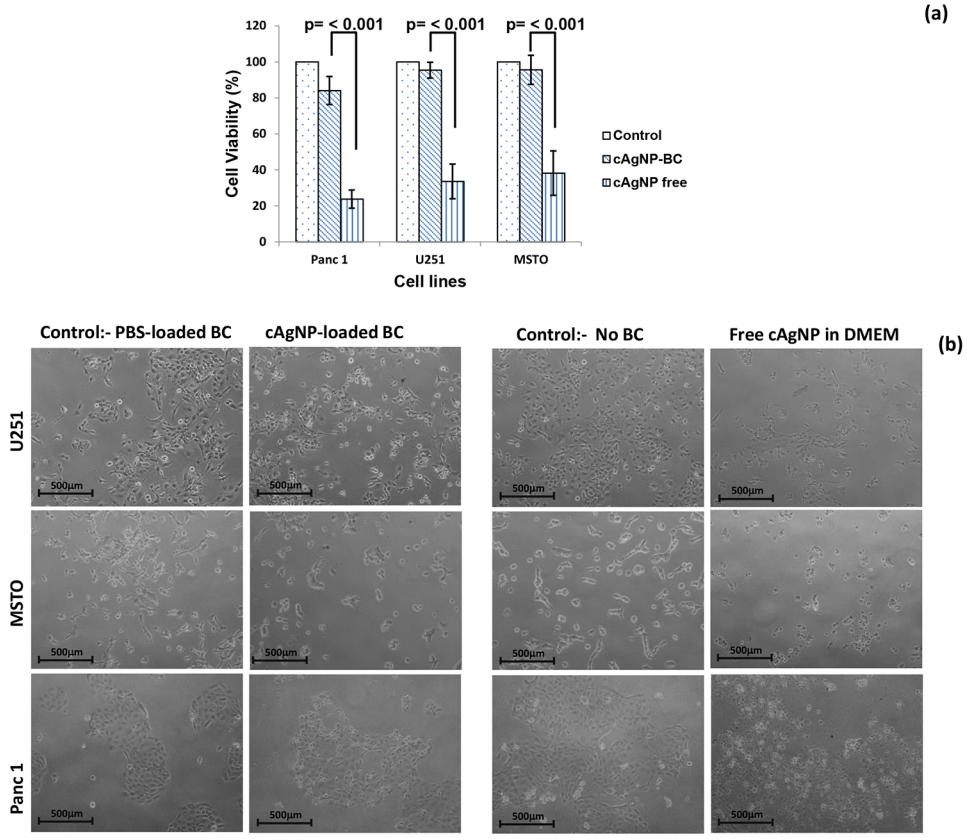

Figure 4. Cytocompatibility test results. (a) Bar graph showing the cell viability (%) after 24 h exposure to cAgNP-loaded BC and free cAgNP (equivalent amount) (n = 8). Representative photomicrographs of cells (10× magnification) after exposure to cAgNP-loaded BC and free cAgNP for 24 h.

and capping properties in cAgNP synthesis, CUR:HPβCD has been demonstrated to have wound-healing properties.[22] The excess of CUR inclusion complex in cAgNP-loaded BC may deliver additional benefits contributing to wound healing.

Morphology and size of nanoparticles was also determined in the SEM photomicrographs (Figure 2d). The average diameter was in the range of 37.2−65.1 nm, and most of the nanoparticles appeared spherical. These results are in accordance with TEM results discussed in the section above.

Energy-Dispersive X-ray (EDX) Analysis. The elemental analysis was carried out by EDX studies. The results confirmed that BC (neat) is composed mainly of carbon and oxygen which is in accordance with our previously reported data.[33] In addition to carbon and oxygen, detection of silver in the EDX spectra of cAgNP-loaded BC (test) confirmed nanoparticle loading in the test samples (Figure 3).

Moisture Content (M_c). BC hydrogels have been reported to have a unique property of resistance to degradation despite considerable moisture content which is several times its dry mass.[14] This strength is contributed by its cross-linked fiber network structure. In the current study, the moisture content of neat BC and cAgNP-loaded BC hydrogels was evaluated. The results confirmed that neat BC pellicles imbibed 99.68 ± 0.09% (v/w) (n = 3) water, which is in accordance with previously reported data (>99.5%) for neat BC hydrogels.[20,22] Moreover, the study on cAgNP-loaded BC revealed that the moisture content in these hydrogels was 98.86 ± 0.04% (n = 3). These findings indicate that the difference in the mass of neat BC and cAgNP-loaded BC is contributed by cAgNP and CUR:HPβCD that gets physically trapped in the fiber network of BC during the loading process.

The high moisture content in BC can confer many benefits such as increased malleability, soft texture, and creating a moist environment with increased dissolved oxygen to facilitate aerobic conditions at the wound-dressing interface. In addition, these hydrogels may ease removal of the dressing, reduce pain sensation and therefore improve patient comfort. These features have been reported to facilitate the wound-healing process,[15,21,57,58] and therefore, BC has attracted increased interest in the wound-care sector.

Cytocompatibility (*In Vitro* Study). The cytocompatible nature of BC is well documented in the literature.[20−22,59] It is one of the many intrinsic features that has resulted in BC-based proprietary products like Dermafill, Biofill, XCell, and Gengiflex.[57,60−62] In this study, the cytocompatibility of cAgNP-loaded BC hydrogels was evaluated using three different mammalian cell lines. The cytotoxicity as determined by MTT assay revealed that cAgNP-loaded BC is cytocompatible as all the tested cell lines demonstrated good survival rate (Figure 4a).

Furthermore, we compared the cytocompatibility of free cAgNP to cAgNP-loaded BC on U251, MSTO and Panc 1 cell lines. The results demonstrated that free cAgNP had a cytotoxic effect on all the tested cell lines, resulting in lower cell viability compared with cAgNP-loaded in BC (p < 0.001) (Figure 4a,b). These results suggest that BC controls the release of cAgNP thus minimizing the cytotoxic effect on the mammalian cells. These findings support the potential

https://dx.doi.org/10.1021/acs.biomac.9b01724
Biomacromolecules 2020, 21, 1802−1811

application of cAgNP-loaded BC for wound management as hydrogel dressings.

Hemocompatibility. Hemocompatibility is an important property for biomedical applications of a material. BC has been reported to be hemocompatible; hence, it has been used in proprietary wound dressings.[20,63,64] In the current study, cAgNPs were prepared in deionized water; hence, the hypothesis was drawn that cAgNP-loaded BC hydrogels may have hemolytic properties. The test results revealed that cAgNP-loaded BC hydrogels have a percentage hemolysis of 6.85 ± 1.12% (n = 6). According to the ASTM F756 standards hemolytic indices, this range is over the threshold value of 5% hence cAgNP-loaded BC hydrogels would be classified as a hemolytic material.[65] The higher hemolysis (%) of the tested hydrogels could be attributed to the use of deionized water instead of the isotonic solution for the synthesis of cAgNP.

In the case of a chronic wound, there could be necrotic tissue or slough at the wound bed, and hence, the hemolytic behavior of these hydrogels may be minimal. Further research on the production of AgNP using CUR:HPβCD dissolved in isotonic solution may improve hemocompatibility of these hydrogels.

Antimicrobial Study. Invasion of opportunistic microbes could impair wound healing, leading to chronic nonhealing wounds.[6,66] Silver nanoparticles have been intensively studied as antimicrobial agents.[40,49,53] Different mechanisms of action of AgNPs have been proposed as their antibacterial and antifungal effect is not completely known.[67] In bacteria, AgNPs have the ability to increase the permeability of the cell membrane, interfere with DNA replication, denature bacterial proteins, and release silver ions inside the bacterial cell.[49,67] The antifungal action of silver nanoparticles are thought to increase the reactive oxygen species within the fungal cell and increase membrane permeability resulting in cell death.[68]

In the current study, PBS-loaded BC, HPβCD-loaded BC, and cAgNP-loaded BC hydrogels were tested against *P. aeruginosa*, *S. aureus*, and *C. auris* using the disc diffusion assay at 24 h. PBS-loaded BC and HPβCD-loaded BC did not exhibit antimicrobial activity; however, cAgNP-loaded BC demonstrated significant antimicrobial activity (p < 0.001) against all three of the tested microbial strains (Figure 5).

These results confirm the broad spectrum antimicrobial activity of cAgNP-loaded in BC. Moreover, it is apparent that cAgNP-loaded in BC has stronger antimicrobial activity (Figure 5) against *P. aeruginosa* as compared with *S. aureus* (p < 0.001). This could be explained by the difference in the cell structure of Gram-positive and Gram-negative bacteria.

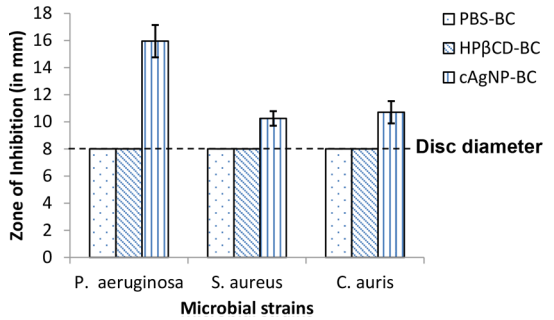

Figure 5. Antimicrobial disc diffusion assay results for PBS-loaded BC, HPβCD-loaded BC, and cAgNP-loaded BC against *P. aeruginosa*, *S. aureus*, and *C. auris* at 24 h (n = 10; error bars = SD).

AgNPs have been reported to have the ability to separate cytoplasm from the bacterial cell wall (plasmolysis effect) leading to cell death in *P. aeruginosa*. In *S. aureus*, AgNPs act differently and cause the bacterial cell death by inhibiting the cell wall synthesis.[49,67,69]

Antioxidant Activity of cAgNP by DPPH Assay. Oxidative stress at the wound site may interfere with the healing process;[70] hence, a wound dressing with antioxidant properties along with antimicrobial activity may prove to be beneficial.[71] CUR has been reported to have healing properties including antimicrobial and antioxidant activities. It has been previously demonstrated that these properties were preserved in the inclusion complex of CUR in HPβCD.[22]

In the current study, cAgNP were successfully prepared using CUR:HPβCD as reducing and stabilizing agent. The percent antioxidant effect (% E) for aqueous cAgNP colloidal suspension against DPPH was determined to be 76.65 ± 3.21% (n = 6). The test results confirmed that silver nitrate and HPβCD does not have antioxidant activity, which is in accordance with previously reported findings.[22] These results confirmed that colloidal cAgNP aqueous medium produced using CUR:HPβCD has antioxidant activity, and when it is loaded in BC to produce hydrogels, it could prove to be beneficial in wound-healing process.

Transparency Test. Monitoring of wound-healing process is vital from a clinical perspective.[72−74] Routinely, this involves the removal of a dressing which can disturb the granulating tissue and could cause trauma to the wound. A dressing with the feature enabling noninvasive monitoring could be beneficial in wound healing.

The transparent nature of BC has already been reported,[22] and in this study, PBS-loaded BC hydrogels reconfirmed these findings (Figure 6a). In this study, the transparency property of

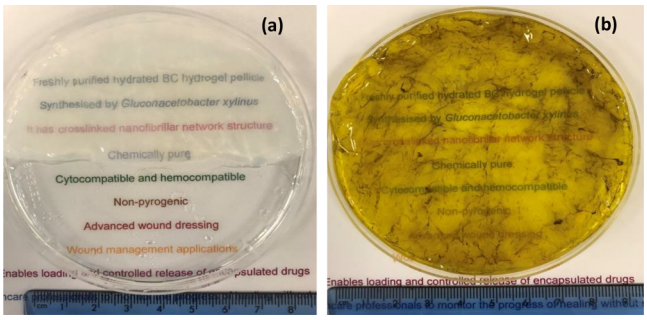

Figure 6. Photomicrographs with the visual appearance of (a) BC loaded with PBS (b) cAgNP-loaded BC hydrogel pellicle.

cAgNP-loaded BC was evaluated by reading the text in different colors on white laminated paper sheet through the test hydrogels. The results (Figure 6b) demonstrate cAgNP-loaded BC hydrogels allow monitoring the wound without the need for removal of the dressing. This transparency testing is a simulation study, and in order to confirm the results, clinical validation would be required and could be evaluated using *in vivo* animal models.

CONCLUSIONS

The development of advanced polymeric materials requires precise evaluation of structure, properties, and behavior to avoid potential failures of the commercial products manufactured from them. The current study demonstrates the

https://dx.doi.org/10.1021/acs.biomac.9b01724
Biomacromolecules 2020, 21, 1802−1811

production and both physicochemical and *in vitro* characterization of cAgNP-loaded BC hydrogels. It also increases efficiency and minimizes the potential failure of precisely structured biomaterials before, during, and after specific applications. The results confirmed that cAgNPs were successfully synthesized, following the green chemistry approach using CUR:HPβCD and loaded in BC to produce hydrogels with a potential wound-dressing application. These hydrogels demonstrated broad-spectrum antimicrobial activity along with antioxidant properties. Moreover, the hydrogels showed cytocompatibility with the tested cell lines. The high moisture content and the good level of transparency further advocate their potential application in the management of chronic wounds with high microbial bioburden.

AUTHOR INFORMATION

Corresponding Authors

Abhishek Gupta − *School of Pharmacy, Faculty of Science and Engineering and Research Institute in Healthcare Science, Faculty of Science and Engineering, University of Wolverhampton, WV1 1LY Wolverhampton, U.K.;* orcid.org/0000-0001-7901-1818; Email: a.gupta@wlv.ac.uk

Marek Kowalczuk − *Centre of Polymer and Carbon Materials, Polish Academy of Sciences, 41-819 Zabrze, Poland;* orcid.org/0000-0002-2877-7466; Email: marek.kowalczuk@cmpw-pan.edu.pl

Iza Radecka − *Wolverhampton School of Sciences, Faculty of Science and Engineering and Research Institute in Healthcare Science, Faculty of Science and Engineering, University of Wolverhampton, WV1 1LY Wolverhampton, U.K.;* orcid.org/0000-0003-3257-8803; Email: I.Radecka@wlv.ac.uk

Authors

Sophie M. Briffa − *School of Geography, Earth and Environmental Sciences, University of Birmingham, B15 2TT Birmingham, U.K.*

Sam Swingler − *Wolverhampton School of Sciences, Faculty of Science and Engineering, University of Wolverhampton, WV1 1LY Wolverhampton, U.K.*

Hazel Gibson − *Wolverhampton School of Sciences, Faculty of Science and Engineering and Research Institute in Healthcare Science, Faculty of Science and Engineering, University of Wolverhampton, WV1 1LY Wolverhampton, U.K.*

Vinodh Kannappan − *Research Institute in Healthcare Science, Faculty of Science and Engineering, University of Wolverhampton, WV1 1LY Wolverhampton, U.K.*

Grazyna Adamus − *Centre of Polymer and Carbon Materials, Polish Academy of Sciences, 41-819 Zabrze, Poland*

Claire Martin − *Department of Biological Sciences, School of Sciences and the Environment, University of Worcester, WR1 3AS Worcester, U.K.;* orcid.org/0000-0002-5497-4594

Complete contact information is available at: https://pubs.acs.org/10.1021/acs.biomac.9b01724

Notes

The authors declare no competing financial interest.

ACKNOWLEDGMENTS

The authors would like to thank Professor Wang Weiguang and his team for their kind assistance. Abhishek Gupta would like to thanks the School of Pharmacy at the University of Wolverhampton for the support towards his Ph.D. research. This paper is partly supported by European Union's Horizon 2020 research and innovation programme under the Marie Skłodowska-Curie grant agreement No 872152, project GREEN-MAP.

REFERENCES

(1) James, G. A.; Swogger, E.; Wolcott, R.; Pulcini, E. d.; Secor, P.; Sestrich, J.; Costerton, J. W.; Stewart, P. S. Biofilms in chronic wounds. *Wound Repair and Regeneration* **2008**, *16*, 37−44.

(2) Duckworth, P. F.; Rowlands, R. S.; Barbour, M. E.; Maddocks, S. E. A novel flow-system to establish experimental biofilms for modelling chronic wound infection and testing the efficacy of wound dressings. *Microbiol. Res.* **2018**, *215*, 141−147.

(3) Bou Haidar, N.; Marais, S.; Dé, E.; Schaumann, A.; Barreau, M.; Feuilloley, M. G. J.; Duncan, A. C. Chronic wound healing: A specific antibiofilm protein-asymmetric release system. *Mater. Sci. Eng., C* **2020**, *106*, 110130.

(4) Xia, G.; Zhai, D.; Sun, Y.; Hou, L.; Guo, X.; Wang, L.; Wang, F.; Li, Z. Preparation of a novel asymmetric wettable chitosan-based sponge and its role in promoting chronic wound healing. *Carbohydr. Polym.* **2020**, *227*, 115296.

(5) Wu, Y.; Cheng, N.; Cheng, C. Biofilms in Chronic Wounds: Pathogenesis and Diagnosis. *Trends Biotechnol.* **2019**, *37*, 505−517.

(6) Williams, H.; Campbell, L.; Crompton, R. A.; Singh, G.; McHugh, B. J.; Davidson, D. J.; McBain, A. J.; Cruickshank, S. M.; Hardman, M. J. Microbial Host Interactions and Impaired Wound Healing in Mice and Humans: Defining a Role for BD14 and NOD2. *J. Invest. Dermatol.* **2018**, *138*, 2264−2274.

(7) Lipsky, B. A.; Holroyd, K. J.; Zasloff, M. Michael Zasloff Topical versus Systemic Antimicrobial Therapy for Treating Mildly Infected Diabetic Foot Ulcers: A Randomized, Controlled, Double-Blinded, Multicenter Trial of Pexiganan Cream. *Clin. Infect. Dis.* **2008**, *47*, 1537−1545.

(8) Namviriyachote, N.; Lipipun, V.; Akkhawattanangkul, Y.; Charoonrut, P.; Ritthidej, G. C. Development of polyurethane foam dressing containing silver and asiaticoside for healing of dermal wound. *Asian J. Pharm. Sci.* **2019**, *14*, 63−77.

(9) Winter, G. D. Formation of the Scab and the Rate of Epithelization of Superficial Wounds in the Skin of the Young Domestic Pig. *Nature* **1962**, *193*, 293−294.

(10) Xue, H.; Hu, L.; Xiong, Y.; Zhu, X.; Wei, C.; Cao, F.; Zhou, W.; Sun, Y.; Endo, Y.; Liu, M.; Liu, G.; Liu, Y.; Liu, J.; Abududilibaier, A.; Chen, L.; Yan, C.; Mi, B. Quaternized chitosan-Matrigel-polyacrylamide hydrogels as wound dressing for wound repair and regeneration. *Carbohydr. Polym.* **2019**, *226*, 115302.

(11) Tao, G.; Wang, Y.; Cai, R.; Chang, H.; Song, K.; Zuo, H.; Zhao, P.; Xia, Q.; He, H. Design and performance of sericin/poly(vinyl alcohol) hydrogel as a drug delivery carrier for potential wound dressing application. *Mater. Sci. Eng., C* **2019**, *101*, 341−351.

(12) Koehler, J.; Brandl, F. P.; Goepferich, A. M. Hydrogel wound dressings for bioactive treatment of acute and chronic wounds. *Eur. Polym. J.* **2018**, *100*, 1−11.

(13) Gupta, A.; Kowalczuk, M.; Heaselgrave, W.; Britland, S. T.; Martin, C.; Radecka, I. The production and application of hydrogels for wound management: A review. *Eur. Polym. J.* **2019**, *111*, 134−151.

(14) Costa, A. F. S.; Almeida, F. C. G.; Vinhas, G. M.; Sarubbo, L. A. Production of Bacterial Cellulose by *Gluconacetobacter hansenii* Using Corn Steep Liquor As Nutrient Sources. *Front. Microbiol.* **2017**, *8*, 2027.

(15) Jiji, S.; Udhayakumar, S.; Rose, C.; Muralidharan, C.; Kadirvelu, K. Thymol enriched bacterial cellulose hydrogel as effective material for third degree burn wound repair. *Int. J. Biol. Macromol.* **2019**, *122*, 452−460.

(16) Wichai, S.; Chuysinuan, P.; Chaiarwut, S.; Ekabutr, P.; Supaphol, P. Development of bacterial cellulose/alginate/chitosan composites incorporating copper (II) sulfate as an antibacterial wound dressing. *J. Drug Delivery Sci. Technol.* **2019**, *51*, 662−671.

(17) Faisul Aris, F. A.; Mohd Fauzi, F. N. A.; Tong, W. Y.; Syed Abdullah, S. S. Interaction of silver sulfadiazine with bacterial cellulose via *ex-situ* modification method as an alternative diabetic wound healing. *Biocatal. Agric. Biotechnol.* **2019**, *21*, 101332.
(18) Khosravi, K.; Koller, M.; Akramzadeh, N.; Mortazavian, A. M. Bacterial nanocellulose: biosynthesis and medical application. *Biointerface Res. Appl. Chem.* **2016**, *6*, 1511−1516.
(19) Abeer, M. M.; Mohd Amin, M. C. I.; Martin, C. A review of bacterial cellulose-based drug delivery systems: their biochemistry, current approaches and future prospects. *J. Pharm. Pharmacol.* **2014**, *66*, 1047−1061.
(20) Gupta, A.; Low, W. L.; Britland, S. T.; Radecka, I.; Martin, C. Physicochemical characterisation of biosynthetic bacterial cellulose as a potential wound dressing material. *Br. J. Pharmacol.* **2018**, *2*, S37−S38.
(21) Zmejkoski, D.; Spasojević, D.; Orlovska, I.; Kozyrovska, N.; Soković, M.; Glamočlija, J.; Dmitrović, S.; Matović, B.; Tasić, N.; Maksimović, V.; Sosnin, M.; Radotić, K. Bacterial cellulose-lignin composite hydrogel as a promising agent in chronic wound healing. *Int. J. Biol. Macromol.* **2018**, *118*, 494−503.
(22) Gupta, A.; Keddie, D. J.; Kannappan, V.; Gibson, H.; Khalil, I. R.; Kowalczuk, M.; Martin, C.; Shuai, X.; Radecka, I. Production and characterisation of bacterial cellulose hydrogels loaded with curcumin encapsulated in cyclodextrins as wound dressings. *Eur. Polym. J.* **2019**, *118*, 437−450.
(23) Kowalczuk, M. M. Forensic Engineering of Advanced Polymeric Materials. *Mathews J. Forensic Research* **2017**, *1*, No. e001.
(24) Kean, R.; Ramage, G. Combined Antifungal Resistance and Biofilm Tolerance: the Global Threat of *Candida auris*. *mSphere* **2019**, *4*, No. e00458-19.
(25) Ciric, L. *Candida auris: The new superbug on the block*. BBC. [online] Available at: https://www.bbc.co.uk/news/health-49170866, 2019.
(26) Speare-Cole, R. *Candida auris*: Eight Britons who died in UK hospitals were infected with Japanese super-fungus. *Evening Standard*. [online] Available at: https://www.standard.co.uk/news/uk/eight-britons-who-died-in-hospital-were-infected-with-japanese-superfungus-a4128901.html **2019**.
(27) Osei Sekyere, J. *Candida auris*: A systematic review and meta-analysis of current updates on an emerging multidrug-resistant pathogen. *MicrobiologyOpen* **2018**, *7*, No. e00578.
(28) Lockhart, S. *Candida auris* and multidrug resistance: Defining the new normal. *Fungal Genet. Biol.* **2019**, *131*, 103243.
(29) Vallabhaneni, S.; Jackson, B.; Chiller, T. *Candida auris*: An Emerging Antimicrobial Resistance Threat. *Ann. Intern. Med.* **2019**, *171*, 432−433.
(30) Arikan-Akdagli, S.; Ghannoum, M.; Meis, J. Antifungal Resistance: Specific Focus on Multidrug Resistance in *Candida auris* and Secondary Azole Resistance in Aspergillus fumigatus. *J. Fungi* **2018**, *4*, 129−142.
(31) Gohlar, G.; Hughes, S. How to improve antifungal stewardship. *Pharmaceutical J.* **2019**, *303*, 7927.
(32) Srivastava, V.; Singla, R.; Dubey, A. Emerging Virulence, Drug Resistance and Future Anti-fungal Drugs for Candida Pathogens. *Curr. Top. Med. Chem.* **2018**, *18*, 759−778.
(33) Gupta, A.; Low, W. L.; Radecka, I.; Britland, S. T.; Mohd Amin, M. C. I.; Martin, C. Characterisation and *in vitro* antimicrobial activity of biosynthetic silver-loaded bacterial cellulose hydrogels. *J. Microencapsulation* **2016**, *33*, 725−734.
(34) Melaiye, A.; Youngs, W. J. Silver and its application as an antimicrobial agent. *Expert Opin. Ther. Pat.* **2005**, *15*, 125−130.
(35) Brandt, O.; Mildner, M.; Egger, A. E.; Groessl, M.; Rix, U.; Posch, M.; Keppler, B. K.; Strupp, C.; Mueller, B.; Stingl, G. Nanoscalic silver possesses broad-spectrum antimicrobial activities and exhibits fewer toxicological side effects than silver sulfadiazine. *Nanomedicine* **2012**, *8*, 478−488.
(36) Parveen, A.; Kulkarni, N.; Yalagatti, M.; Abbaraju, V.; Deshpande, R. In vivo efficacy of biocompatible silver nanoparticles cream for empirical wound healing. *J. Tissue Viability* **2018**, *27*, 257−261.
(37) Ravindran, J.; Arumugasamy, V.; Baskaran, A. Wound healing effect of silver nanoparticles from *Tridax procumbens* leaf extracts on *Pangasius* hypophthalmus. *Wound Medicine* **2019**, *27*, 100170.
(38) Ahsan, A.; Farooq, M. A. Therapeutic potential of green synthesized silver nanoparticles loaded PVA hydrogel patches for wound healing. *J. Drug Delivery Sci. Technol.* **2019**, *54*, 101308.
(39) Keshari, A. K.; Srivastava, R.; Singh, P.; Yadav, V. B.; Nath, G. Antioxidant and antibacterial activity of silver nanoparticles synthesized by *Cestrum nocturnum*. *J. Ayurveda and Integrative Medicine* **2018**, 1−8.
(40) Alsammarraie, F. K.; Wang, W.; Zhou, P.; Mustapha, A.; Lin, M. Green synthesis of silver nanoparticles using turmeric extracts and investigation of their antibacterial activities. *Colloids Surf., B* **2018**, *171*, 398−405.
(41) Hemmati, S.; Rashtiani, A.; Zangeneh, A.; Zangeneh, M. M.; Mohammadi, P.; Veisi, H. Green synthesis and characterization of silver nanoparticles using Fritillaria flower extract and their antibacterial activity against some human pathogens. *Polyhedron* **2019**, *158*, 8−14.
(42) Akbik, D.; Ghadiri, M.; Chrzanowski, W.; Rohanizadeh, R. Curcumin as a wound healing agent. *Life Sci.* **2014**, *116*, 1−7.
(43) Song, Z.; Wu, Y.; Wang, H.; Han, H. Synergistic antibacterial effects of curcumin modified silver nanoparticles through ROS-mediated pathways. *Mater. Sci. Eng., C* **2019**, *99*, 255−263.
(44) Pandit, R.; Gaikwad, S.; Agarkar, G.; Gade, A.; Rai, M. Curcumin nanoparticles: physico-chemical fabrication and its *in vitro* efficacy against human pathogens. *3 Biotech* **2015**, *5*, 991−997.
(45) Abdulwahab, F.; Henari, F. Z.; Cassidy, S.; Winser, K. Synthesis of Au, Ag, Curcumin Au/Ag, and Au-Ag Nanoparticles and Their Nonlinear Refractive Index Properties. *J. Nanomater.* **2016**, *2016*, 5356404.
(46) Yang, X. X.; Li, C. M.; Huang, C. Z. Curcumin modified silver nanoparticles for highly efficient inhibition of respiratory syncytial virus infection. *Nanoscale* **2016**, *8*, 3040−3048.
(47) Murugesan, K.; Koroth, J.; Srinivasan, P. P.; Singh, A.; Mukundan, S.; Karki, S. S.; Choudhary, B.; Gupta, C. M. Effects of green synthesised silver nanoparticles (ST06-AgNPs) using curcumin derivative (ST06) on human cervical cancer cells (HeLa) in vitro and EAC tumor bearing mice models. *Int. J. Nanomed.* **2019**, *14*, 5257−5270.
(48) Khan, M. J.; Shameli, K.; Sazili, A. Q.; Selamat, J.; Kumari, S. Rapid Green Synthesis and Characterization of Silver Nanoparticles Arbitrated by Curcumin in an Alkaline Medium. *Molecules* **2019**, *24*, 719.
(49) Lyu, Y.; Yu, M.; Liu, Q.; Zhang, Q.; Liu, Z.; Tian, Y.; Li, D.; Changdao, M. Synthesis of silver nanoparticles using oxidized amylose and combination with curcumin for enhanced antibacterial activity. *Carbohydr. Polym.* **2020**, *230*, 115573.
(50) Shameli, K.; Ahmad, M. B.; Zamanian, A.; Sangpour, P.; Shabanzadeh, P.; Abdollahi, Y.; Mohsen, Z. Green biosynthesis of silver nanoparticles using *Curcuma longa* tuber powder. *Int. J. Nanomed.* **2012**, *7*, 5603−5610.
(51) Hestrin, S.; Schramm, M. Synthesis of cellulose by *Acetobacter xylinum*. II. Preparation of freeze-dried cells capable of polymerizing glucose to cellulose. *Biochem. J.* **1954**, *58*, 345.
(52) Liu, D.; Cao, Y.; Qu, R.; Gao, G.; Chen, S.; Zhang, Y.; Wu, M.; Ma, T.; Li, G. Production of bacterial cellulose hydrogels with tailored crystallinity from *Enterobacter* sp. FY-07 by the controlled expression of colanic acid synthetic genes. *Carbohydr. Polym.* **2019**, *207*, 563−570.
(53) Sathishkumar, M.; Sneha, K.; Yun, Y. Immobilization of silver nanoparticles synthesized using *Curcuma longa* tuber powder and extract on cotton cloth for bactericidal activity. *Bioresour. Technol.* **2010**, *101*, 7958−7965.
(54) Jalili Tabaii, M.; Emtiazi, G. Transparent nontoxic antibacterial wound dressing based on silver nano particle/bacterial cellulose nano

composite synthesized in the presence of tripolyphosphate. *J. Drug Delivery Sci. Technol.* **2018**, *44*, 244−253.
(55) Srivatsan, K. V.; Duraipandy, N.; Begum, S.; Lakra, R.; Ramamurthy, U.; Korrapati, P. S.; Kiran, M. S. Effect of curcumin caged silver nanoparticle on collagen stabilization for biomedical applications. *Int. J. Biol. Macromol.* **2015**, *75*, 306−315.
(56) Wu, J.; Zheng, Y.; Song, W.; Luan, J.; Wen, X.; Wu, Z.; Chen, X.; Wang, Q.; Guo, S. *In situ* synthesis of silver-nanoparticles/bacterial cellulose composites for slow-released antimicrobial wound dressing. *Carbohydr. Polym.* **2014**, *102*, 762−771.
(57) Portela, R.; Leal, C. R.; Almeida, P. L.; Sobral, R. G. Bacterial cellulose: a versatile biopolymer for wound dressing applications. *Microb. Biotechnol.* **2019**, *12*, 586−610.
(58) Khalid, A.; Ullah, H.; Ul-Islam, M.; Khan, R.; Khan, S.; Ahmad, F.; Khan, T.; Wahid, F. Bacterial cellulose-TiO2 nanocomposites promote healing and tissue regeneration in burn mice model. *RSC Adv.* **2017**, *7*, 47662−47668.
(59) Pértile, R. A. N.; Moreira, S.; Gil da Costa, R. M.; Correia, A.; Guãrdao, L.; Gartner, F.; Vilanova, M.; Gama, M. Bacterial Cellulose: Long-Term Biocompatibility Studies. *J. Biomater. Sci., Polym. Ed.* **2012**, *23*, 1339−1354.
(60) Lee, K.; Buldum, G.; Mantalaris, A.; Bismarck, A. More Than Meets the Eye in Bacterial Cellulose: Biosynthesis, Bioprocessing, and Applications in Advanced Fiber Composites. *Macromol. Biosci.* **2014**, *14*, 10−32.
(61) Lopes, T. D.; Riegel-Vidotti, I. C.; Grein, A.; Tischer, C. A.; Faria-Tischer, P. C. d. S. Faria-Tischer, Paula Cristina de Sousa Bacterial cellulose and hyaluronic acid hybrid membranes: Production and characterization. *Int. J. Biol. Macromol.* **2014**, *67*, 401−408.
(62) Moniri, M.; Boroumand Moghaddam, A.; Azizi, S.; Abdul Rahim, R.; Bin Ariff, A.; Zuhainis Saad, W.; Navaderi, M.; Mohamad, R. Production and Status of Bacterial Cellulose in Biomedical Engineering. *Nanomaterials* **2017**, *7*, 257.
(63) Andrade, F. K.; Silva, J. P.; Carvalho, M.; Castanheira, E. M. S.; Soares, R.; Gama, M. Studies on the hemocompatibility of bacterial cellulose. *J. Biomed. Mater. Res., Part A* **2011**, *98A*, 554−566.
(64) Leitão, A. F.; Gupta, S.; Silva, J. P.; Reviakine, I.; Gama, M. Hemocompatibility study of a bacterial cellulose/polyvinyl alcohol nanocomposite. *Colloids Surf., B* **2013**, *111*, 493−502.
(65) Subcommittee F04.16 on Biocompatibility Test Methods. *Standard Practice for Assessment of Hemolytic Properties of Materials*. ASTM F756-17; ASTM International: West Conshohocken, PA, 2017.
(66) Nagoba, B.; Davane, M. Studies on wound healing potential of topical herbal formulations- do we need to strengthen study protocol? *J. Ayurveda and Integrative Medicine* **2019**, *10*, 316−318.
(67) Guzman, M.; Dille, J.; Godet, S. Synthesis and antibacterial activity of silver nanoparticles against gram-positive and gram-negative bacteria. *Nanomedicine* **2012**, *8*, 37−45.
(68) Khatoon, U.; Rao, G.; Mohan, M.; Ramanaviciene, A.; Ramanavicius, A. Comparative study of antifungal activity of silver and gold nanoparticles synthesized by facile chemical approach. *J. Environ. Chem. Eng.* **2018**, *6*, 5837−5844.
(69) Song, H. Y.; Ko, K. K.; Oh, I. H.; Lee, B. T. Fabrication of silver nanoparticles and their antimicrobial mechanisms. *Eur. Cells Mater.* **2006**, *11*, 58−59.
(70) Cano Sanchez, M.; Lancel, S.; Boulanger, E.; Neviere, R. Targeting Oxidative Stress and Mitochondrial Dysfunction in the Treatment of Impaired Wound Healing: A Systematic Review. *Antioxidants* **2018**, *7*, 98.
(71) Ahmed, O. M.; Mohamed, T.; Moustafa, H.; Hamdy, H.; Ahmed, R. R.; Aboud, E. Quercetin and low level laser therapy promote wound healing process in diabetic rats via structural reorganization and modulatory effects on inflammation and oxidative stress. *Biomed. Pharmacother.* **2018**, *101*, 58−73.
(72) Flanagan, M. Wound measurement: can it help us to monitor progression to healing? *J. Wound Care.* **2003**, *12*, 189−194.
(73) Kenworthy, P.; Phillips, M.; Grisbrook, T. L.; Gibson, W.; Wood, F. M.; Edgar, D. W. Monitoring wound healing in minor burns—A novel approach. *Burns* **2018**, *44*, 70−76.
(74) Malone, M.; Schwarzer, S.; Walsh, A.; Xuan, W.; Al Gannass, A.; Dickson, H. G.; Bowling, F. L. Monitoring wound progression to healing in diabetic foot ulcers using three-dimensional wound imaging. *J. Diabetes Complications.* **2020**, *34*, 107471.

https://dx.doi.org/10.1021/acs.biomac.9b01724
Biomacromolecules 2020, 21, 1802−1811